INITIAL SYNCHROSCAN STREAK CAMERA IMAGING AT THE A0 PHOTOINJECTOR*

A.H. Lumpkin and J. Ruan, Fermilab, Batavia, IL U.S.A. 60510

Abstract

At the Fermilab A0 photoinjector facility, bunch-length measurements of the laser micropulse and the e-beam micropulse have been done in the past with a single-sweep module of the Hamamatsu C5680 streak camera with an intrinsic shot-to-shot trigger jitter of 10 to 20 ps. We have upgraded the camera system with the synchroscan module tuned to 81.25 MHz to provide synchronous summing capability with less than 1.5-ps FWHM trigger jitter and a phase-locked delay box to provide phase stability of ~1 ps over 10s of minutes. This allowed us to measure both the UV laser pulse train at 244 nm and the e-beam via optical transition radiation (OTR). Due to the low electron beam energies and OTR signals, we typically summed over 50 micropulses with 1 nC per micropulse. We also did electron beam bunch length vs. micropulse charge measurements to identify a significant e-beam micropulse elongation from 10 to 30 ps (FWHM) for charges from 1 to 4.6 nC. This effect is attributed to space-charge effects in the PC gun as reproduced by ASTRA calculations. Chromatic temporal dispersion effects in the optics were also characterized and will be reported.

INTRODUCTION

The opportunity for a new series of streak camera experiments at the Fermilab A0 photoinjector was recognized in the last year. The enabling upgrade was adding the synchroscan option to the existing C5680 Hamamatsu streak camera mainframe. By locking this module to the 81.25 MHz subharmonic of the rf system, the synchronous summing of micropulses could be done with trigger jitter of <1.5 ps (FWHM) for both the UV drive laser component at 244 nm and the e-beam via optical transition radiation (OTR) measurements [1,2]. The synchronous summing of the low OTR signal from the 15-MeV electron beam micropulses allowed the needed bandpass filters to be utilized to reduce the chromatic temporal dispersion effects inherent to the broadband OTR source and the transmissive optics components. In addition, the C6768 delay module with phase feedback was also acquired, and this stabilized the streak camera sweep relative to the master oscillator so that camera phase drift was much reduced to the ps level over 10s of minutes. This latter feature allowed a series of experiments to be done on the bandwidth effects and transit time effects in the respective transport lines. After characterizing the UV laser bunch length, a series of e-beam experiments on the A0 beamlines was performed. We have measured a significant bunch-length elongation versus micropulse charge for the present conditions and show that this is consistent with ASTRA calculations. We also observed a micropulse slice emittance effect for charges of 4 nC per micropulse. In the course of our experiments, we have done a series of tests on the chromatic temporal dispersion effects for this particular input optics barrel with UV transmitting optics and our optical transport lines. We show our effects our less than that reported at SSRL at PAC07 with optical synchrotron radiation (OSR) [3], but ours still have to be characterized carefully to allow accurate bunch-length measurements using the OTR in our case. Finally, we report measurements of the bunch compression in a double-dogleg transport line as a function of the upstream 9-cell accelerator rf phase.

*Work supported by U.S. Department of Energy, Office of Science, Office of High Energy Physics, under Contract No. DE-AC02-07CH1135.

EXPERIMENTAL BACKGROUND

The tests were performed at the Fermilab A0 photoinjector facility which includes an L-band photocathode (PC) rf gun and a 9-cell SC rf accelerating structure which combine to generate up to 16-MeV electron beams [4]. The drive laser operates at 81.25 MHz although the micropulse structure is usually counted down to 9 MHz. Previous bunch length measurements of the drive laser and e-beam [2] were done with the fast single-sweep module of the Hamamatsu C5680 streak camera with an inherent shot-to-shot trigger jitter of 10 to 20 ps. Such jitter precluded synchronous summing of the short pulses. We have upgraded the camera by acquiring the M5676 synchroscan module tuned to 81.25 MHz with a trigger jitter of less than 1.5 ps (FWHM) and the C6878 phase-locked delay unit which stabilizes the camera phase over 10s of minutes. Due to the low, electron-beam energies and OTR signals, we typically synchronously summed over 50 micropulses with 1 nC per micropulse. The tests were performed in the straight-ahead line where energizing a dipole sends the beam into a final beam dump. The setup includes the upstream corrector magnets, quadrupoles, rf BPM, the YAG:Ce/OTR imaging stations, and the beam dump as schematically shown in Fig. 1. The initial sampling station was chosen at Cross #9, and an optical transport system using flat mirrors and a parabolic mirror brought the light to the streak camera. A short focal length quartz lens was used to focus the beam image more tightly onto the streak camera entrance slit. The quartz-based UV-Vis input optics barrel transferred the slit image to the Hamamatsu C5680 streak camera's photocathode.

Alternatively, the 4-dipoles of the emittance exchange line could be powered and experiments done at an OTR station, Cross #24, after the fourth dipole.

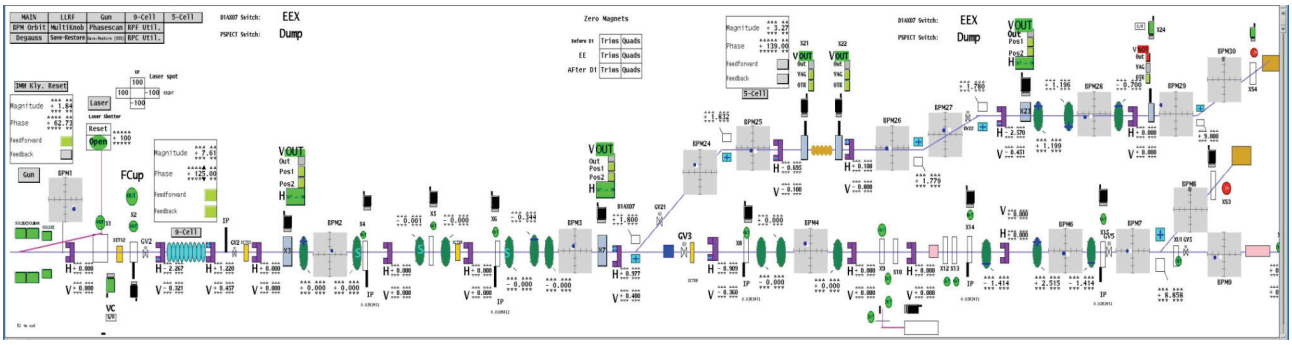

Figure 1: A schematic of the A0 photoinjector test area showing the PC gun, 9-cell cavity, the rf BPMs, the OTR/ODR station, the optics with camera, and the second beamline when the two dogleg dipoles are powered.

A second optical transport line brings the OTR to the streak camera. In the EEX line the bunch compression effects were observed, and the shorter bunches were used to help delineate the chromatic temporal dispersion effects for various band pass, long pass, and short pass filters The OTR converter is an Al-coated optics mirror that is 1.5 mm thick with a zerodur substrate, and is mounted with its surface normal at 45 degrees to the beam direction on a stepper assembly. The assembly provides vertical positioning with an option for a YAG:Ce scintillator crystal position. We still suspect the larger beam sizes may have resulted in incomplete signal collection over angle space. A two-position actuator and a 4-position translation stage were used in the optical path in front of the camera to select band pass filters. The OTR streak readout camera images were recorded with a PCI-compatible video digitizer for both online and offline image analyses. The charge was monitored by an upstream current monitor.

RESOLUTION AND BANDWIDTH EFFECTS

The first step in verifying streak camera operations is to determine the static spread function contribution to temporal resolution. This is the vertical beam spot size of the entrance slit mapped through the imaging system when in camera "focus" mode. The major contribution is the slit height itself for values larger than 30 µm or so. In our early experiments with 10-50 nC of charge integrated in the micropulse sum, we used a slit height of 80 µm, which resulted in a limiting vertical spot size of 9 pixels. The limiting resolution is then found by multiplying this by the sweep-speed calibration factor. We did a careful determination of the two fastest ranges, range 2 and range 1 by using a laser pulse-stacker configuration. By splitting the laser beam energy, we could separately delay one pulse relative to the other by a set of movable mirrors. We then tracked the observed pulse separations in the streak camera images. A plot of the observed time separations is shown in Fig. 2 for range 2 and Fig. 3 for range 1. The reciprocals of the fitted slopes gave us 1.55 ps/pixel and 0.32 ps/pixel, respectively. This means our initial resolution terms were 14.0 ps and 2.9 ps (FWHM), respectively. In the second series of experiments we reduced the slit height to 40 µm with a corresponding vertical spot size of 4.7 pixels (FWHM). This then gives us resolution terms of 7.3 ps and 1.50 ps (FWHM), respectively, for range 2 and range 1. This was needed for the bunch compression tests particularly.

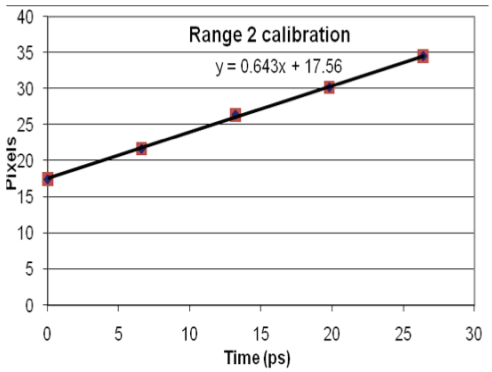

Figure 2: Calibration of the streak camera Range 2 using the laser pulse stacker. The separation of the split laser beam pulses was adjusted with the mirror spacing.

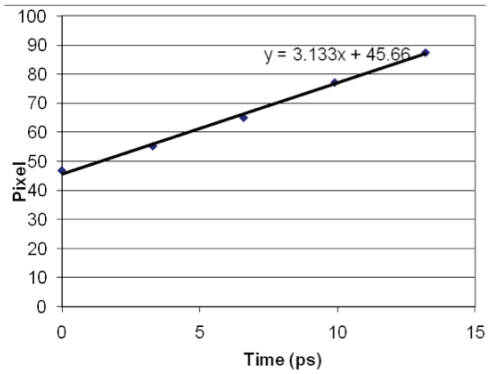

Figure 3: Calibration of the streak camera Range 1 using the laser pulse stacker. The separation of the split laser beam pulses was adjusted with the mirror spacing.

One of the practical issues we addressed was the chromatic temporal dispersion that occurred for the broadband OTR light as it was transported through the

transmissive components of the optical transport line. Since the input optics barrel of the streak camera was actually UV transmitting, it consisted of quartz optical components. This material has less variation of index of refraction with wavelength than flint glass or other materials used in the other standard Hamamatsu input optics, but still results in a measurable effect that limits effective temporal resolution with broadband light. Our effect was shown to be smaller than the SSRL setup of 0.2 ps/nm reported at PAC07 [3]. The basic concept is expressed by the simple relationship for the transit-time change, $\Delta t = L\,(v_{g2}-v_{g1})/(v_{g1} \times v_{g2})$, due to the difference in group velocities v_{g1} and v_{g2} for two wavelengths through a characteristic material thickness, L [5].

This effect is represented in Fig. 4 where a 3-ps FWHM actual pulse is shown as arriving at different times for different wavelengths with a 4-ps shift across the bandwidth of the measurement. The resulting superposition of these Gaussian profiles can be fit to a single Gaussian of 4.21 ps (FWHM). In the actual MATLAB model, a series of over 1000 Gaussians was used. In our case the temporal shift was 8 to 9 ps within the 550-nm shortpass filter bandwidth and caused an effective limiting resolution term of about 4.4 pixels (FWHM) for range 2 in quadrature with the static spread function of 4.7 pixels.

We then can calculate the actual pulse length by subtracting from the total observed pulse width in pixels the contributing terms of static spread function, bandwidth, and trigger jitter. Since the jitter term appears to be small compared to our bunch lengths, we have absorbed it into the actual bunch length term for the time being. Then for range 2 and range 1 we would have respectively:

$$\delta t(FWHM) = \sqrt{Pixel^2 - 4.7^2 - 4.4^2} \times 1.55 ps/pixel$$

$$\delta t(FWHM) = \sqrt{Pixel^2 - 4.7^2 - 22^2} \times 0.32 ps/pixel$$

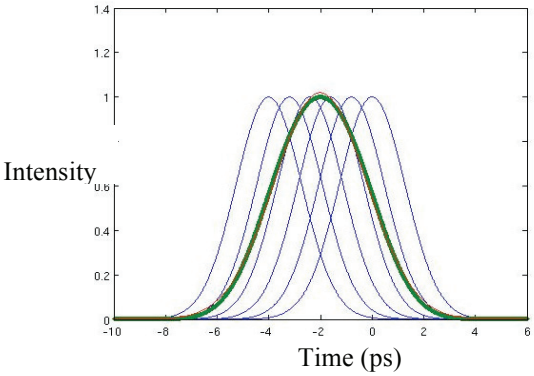

Figure 4: A simple representation of the group velocity dispersion effect on the streak image for a 3-ps FWHM initial pulse and a 4-ps temporal shift in the bandwidth used. The blue curves represent the series of Gaussians time shifted with wavelength. The resultant streak image profile has a 4.21 ps (FWHM) size (green curve).

STREAK CAMERA OTR RESULTS

The experiments were usually initiated by verifying the OTR-deduced spot sizes and centering of the beam on the screen centerline and the downstream rf BPM coordinates. We would optimize the signal transported through the entrance slit of the streak camera while in Focus mode. We then switched to either range 2 or range 1, set the delay for viewing the streak images, and phase locked the delay box.

In the case of the straight-ahead line, we first tried to use larger charges in the micropulse and integrated over 10 pulses. Figure 5 shows the results for both range 2 and range 1 with 5.3 nC per micropulse and 10 micropulses synchronously summed in the image. For these data we actually used a 550 x 40 nm bandpass filter so the bandwidth effects are negligible. After subtracting a larger limiting resolution of 9 ch (FWHM) from each image for this setup, the bunch length was determined as 31± 2ps in range 2 and 32 ± 2 ps in range 1. This was a somewhat larger value than expected so we next did a series of bunch length measurements in which we varied the micropulse charge only. The drive laser bunch length was maintained at about 7.9 ps (FWHM), as verified by a separate streak camera measurement. The results are shown in Fig. 6 where a significant elongation of the e-beam micropulse from 10 to 30 ps occured as we varied the charge/micropulse from 1 nC to 5 nC. For comparison we also show a previous measurement reported in Rodion's dissertation on this photoinjector which has a decidedly different slope [2]. We attribute this difference to the laser spot size being previously reported as 1.77 mm rms compared to the present measured value of 1.15 mm rms. Since the bunch lengths were within 10 % in each case, the space charge effects should be stronger in our data. This is consistent with the ASTRA results (black curve) that simulate our present situation and shown in Fig. 6 as well. The previous ASTRA simulation curve falls very close to the reported experimental data [2].

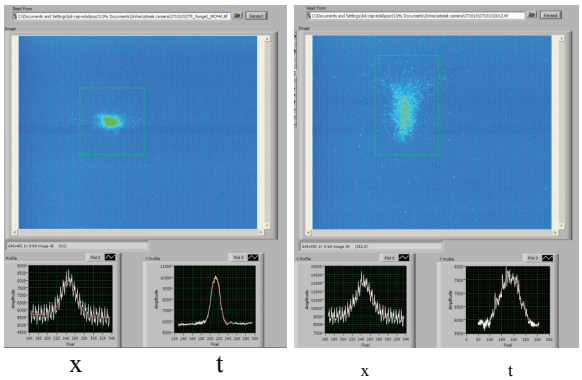

Figure 5: Streak camera image using range 2 (left) and range 1 (right). In the images the vertical axis is the time axis, and the horizontal display axis is the x spatial axis. The bunch length profile is at the lower right of the image and has a width of 32±2 ps (FWHM).

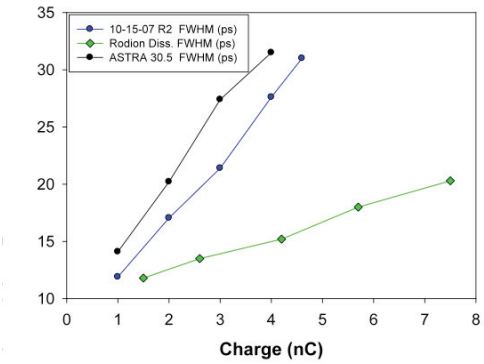

Figure 6: Comparison of the variation of bunch length FWHM with micropulse charge as measured [in Oct. 2007] (blue curve) and as simulated by ASTRA (black curve) and a previous measurement by Rodion (green curve).

As part of these studies we also noted an apparent beam size variation *within* the micropulse time scale as shown in Fig. 7 for a micropulse charge of 4 nC. The observed synchronous sum beam size in the center (green) region of interest (ROI) is about 34.5 ch (FWHM), while it is 50.4 ch at the upper end (red ROI). A beam-size ratio of 1.46 for that portion in the end ROI over the middle ROI was found. The bunch length is about 28 ps (FWHM).

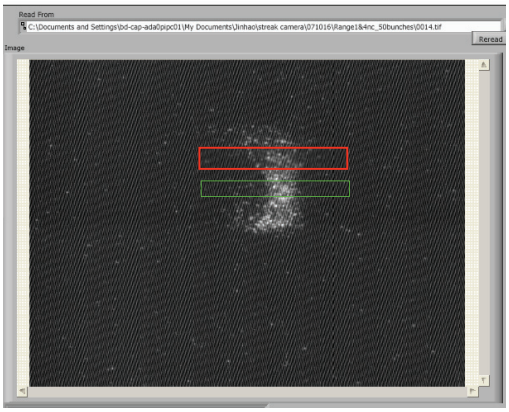

Figure 7: Evidence for slice beam-size effects on the micropulse time scale for a 4-nC micropulse charge. The x beam size sampled at each end of the time profile is about 50% larger than that sampled in the middle (green ROI) of the pulse.

The next series of investigations was done in the other beam line that is setup for emittance exchange experiments [6]. A 5-cell TM_{110} rf superconducting deflector cavity is positioned between two transport doglegs. Compression of the e-beam can be done by proper phasing of the upstream 9-cell cavity. In Fig. 8 we show the results of our initial experiments. The 9-cell rf accelerator phase is varied from 5 degrees off crest to about 25 degrees off crest [7]. The reference phase is 148 degrees in this case. The minimum bunch length is expected at about 21 degrees off crest based on simulations. Due to lower OTR signal transport, we used 100 micropulses of 1 nC per micropulse summed in the images. The bunch length is seen to vary from 22 ps down to 3.8 ps (FWHM) for these conditions. We used both R2 and R1 with the 550 nm short pass filter, and then one additional scan another day was done with the 550 nm LP filter in place with R1. The data were matched in phase at the local minimum. The overlap of points for the different ranges and filters are all in good agreement. This supports the validity of our analysis of the various contributions to resolution.

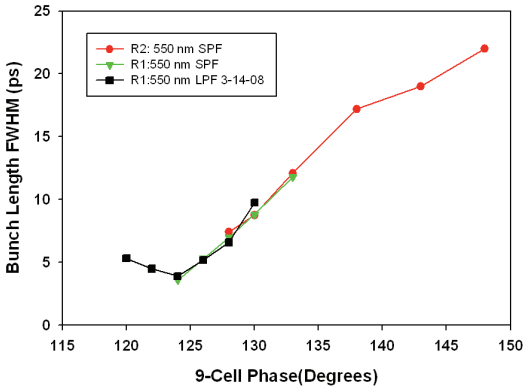

Figure 8: The variation of bunch length with 9-cell phase as measured by the streak camera after the two transport doglegs.

Also the trajectory change with beam energy can be studied via the transit time changes through the doglegs as shown in Fig. 9. The phase-locked streak images allow the change in image time position to be used to track the arrival time change. One can see that a ±1% change in momentum causes an about ±6 ps change, respectively, in transit time through the bends. These data were used to evaluate one of the transport matrix elements of the emittance exchange line.

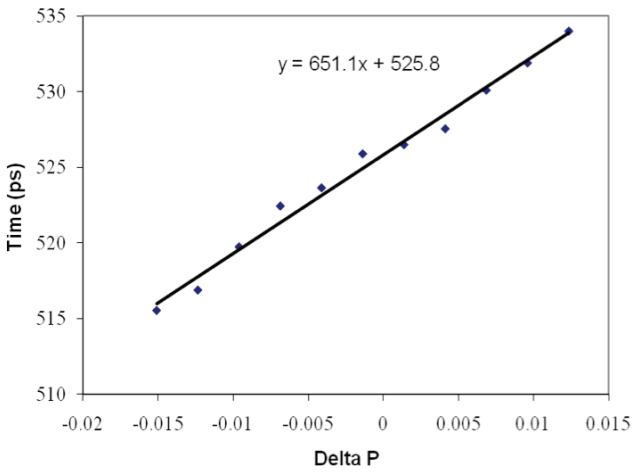

Figure 9: A plot of the change in transit time through the doglegs for different 9-cell rf amplitudes, and hence momentum changes, Delta P.

SUMMARY

In summary, we have extended the investigations on streak camera imaging of the 15-MeV electron beam in the transport lines of the A0 photoinjector using OTR as the conversion mechanism. The enabling technology for these measurements was the synchroscan module installed in the streak camera mainframe combined with the new phaselocked delay box. These allowed synchronous summing of micropulses with much lower jitter than the single sweep unit and with the phase stability locked over 10s of minutes. We were able to measure space-charge effects in the gun, bunch compression effects, transit time effects, and chromatic temporal dispersion effects in our optics. Further investigations are planned on these effects, and a dual sweep unit for the streak camera will be added to the options to explore macropulse time-scale effects.

ACKNOWLEDGEMENTS

The authors acknowledge support from M. Wendt and H. Edwards of Fermilab and A0 technical assistance from J. Santucci, R. Fliller, T. Koeth, and M. Davidsaver.

REFERENCES

[1] Alex H. Lumpkin, "The Next Generation of RF FEL (Free Electron Laser) Diagnostics: Synchroscan and Dual-Sweep Streak Camera Techniques," Nucl. Inst. and Meth. in Phys. Res., A304, 31 (1991).

[2] Tikohoplav Rodion, PhD thesis, "Low Emittance Electron Beam Studies", FERMILAB-THESIS-2006-04.

[3] J.Corbett et al., "Bunch Length Measurements in SPEAR3", Proc. of PAC07, FRPMS065.

[4] R. P. Fliller, H. Edwards, W. Hartung, "Time dependent quantum efficiency and dark current measurements in an RF Photocathode injector with a high quantum efficiency cathode", proc. of PAC05, Knoxville, USA.

[5] H.Staerk, J. Ihlemann, A. Helmbold, "Group Velocity Dispersion: Its Consideration in Picosecond Spectroscopy with Streak Cameras", Laser und Optoelektronik, **28**, 6 (1988) in english.

[6] T. Koeth, L. Bellantoni, D. Edwards, H. Edwards, R. P. Fliller III, " A TM110 Cavity for Longitudinal to Transverse Emittance Exchange", PAC 07, THPAS079, Albuquerque , NM , USA

[7] Ray Fliller (Fermilab, Private communication, Jan. 2008.)